Hindawi Publishing Corporation
Advances in Physical Chemistry
Volume 2012, Article ID 362608, 9 pages
doi:10.1155/2012/362608

Research Article

The N$\cdots$HF Interactions in the X-Pyridazine$\cdots$$(HF)_2$ Complexes: Substituent Effects and Energy Components

Ali Ebrahimi, Mostafa Habibi-Khorassani, Farideh Badichi Akher, and Abdolkarim Farrokhzadeh

Department of Chemistry, University of Sistan and Baluchestan, P.O. Box 98135-674, Zahedan, Iran

Correspondence should be addressed to Ali Ebrahimi, ebrahimi@chem.usb.ac.ir

Received 31 October 2011; Revised 4 January 2012; Accepted 24 January 2012

Academic Editor: Laimutis Bytautas

The effects of substituents on the N$\cdots$HF interactions in the X-pyridazine$\cdots$$(HF)_n$ (X = $N(CH_3)_2$, $NHCH_3$, NH_2, C_2H_5, CH_3, OCH_3, OH, CN, OF, NO_2, F, Br, Cl, and $n = 1, 2$) complexes have been studied at the B3LYP/6-311++G(d,p) level of theory. In all complexes, the binding energies increase for the electron-donating substituents and decrease for the electron-withdrawing substituents. A negative cooperativity is observed for two hydrogen bond interactions. There are meaningful relationships between the Hammett constants and the energy data and the results of population analysis in the binary and ternary complexes. Symmetryadapted perturbation theory (SAPT) analysis was also carried out to unveil the nature of hydrogen bond in the complexes **2** and **3**. The electron-donating substituents increase the magnitude of the SAPT interaction energy components and the electron-withdrawing substituents decrease those components. The highest/lowest change is observed for the E_{exch}/E_{disp} component. The effect of C_2H_5 (or CH_3) on different components is higher than OCH_3 in the complex **2** while the trend is reversed in the complex **3**. It is demonstrated that the electrostatic interaction plays a main role in the interaction, although induction and dispersion interactions are also important.

1. Introduction

The diazine rings are building blocks of many important natural and synthetic compounds [1]. They have been the subject of extensive research, particularly in the pharmaceutical and agrochemical areas due to their broad activities, such as antihypertensive and anti-inflammatory activity [2–5].

The hydrogen bond plays a crucial role in biology, chemistry and related disciplines [6–13]. Cooperativity is an important characteristic of hydrogen bond interactions. The role of hydrogen bond may be modified by the cooperativity of hydrogen bonds in many chemical and biological systems [14–16]. It plays an important role in controlling and regulating the processes occurring in living organisms. Many physical and chemical properties of materials are determined by hydrogen-bonding cooperativity [17–20]. For example, the hydrogen bond cooperativity is relevant for sustaining the stable conformers of biological molecules [21, 22] and constructing the crystal structures [22, 23].

The effects of substituents on the binding energies of the X-pyridazine$\cdots$$(HF)_n$ ($n = 1, 2$) complexes (represented by **1**–**3** in Scheme 1) and the cooperativity of the H-bond interactions have been investigated in the present study. Substituent X is located at position 4 of pyridazine ring, which is meta relative to N_2 in **1** and **2** and para relative to N_1 in **1** and **3**. The relationship between binding energies and the Hammett constants have been studied for binary and ternary complexes. Also, the cooperativity of two hydrogen bond interactions and the strength of interactions have been investigated by the results of atoms in molecules (AIMs) [24], the natural bond orbital (NBO) [25], and molecular electrostatic potential (MEP) analysis. Symmetry-adapted perturbation theory (SAPT) [26] has been employed to determine the physically significant components of the total interaction energies for the complexes **2** and **3**.

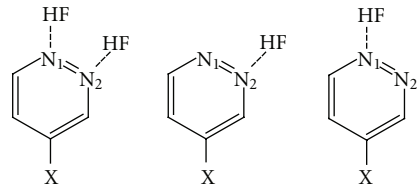

Scheme 1: The X-pyridazine$\cdots$(HF)$_n$ complexes considered in the present work (X = $N(CH_3)_2$, $NHCH_3$, NH_2, C_2H_5, CH_3, OCH_3, OH, CN, OF, NO_2, F, Br, Cl, and $n = 1, 2$).

2. Methods

The geometries of the complexes were fully optimized with the B3LYP [27] method using the 6-311++G(d,p) basis set by the Gaussian 03 program package [28]. The single-point calculations were carried out using the MP2 [29] and PBE1-KCIS [30] methods in conjunction with the 6-311++G(d,p) and aug-cc-pVDZ basis sets. The interaction energies were corrected with the basis set superposition error (BSSE) using the counterpoise method of Boys and Bernardi [31]. The frequency calculations were performed at the B3LYP/6-311++G(d,p) level of theory. The obtained wave functions at the B3LYP/6-311++G(d,p) computational level have been used to analyze the electron density within the AIM methodology by the AIM2000 program [32]. The NBO analysis has been performed using the HF method in conjunction with the 6-311++G(d,p) basis set using the NBO3.1 program in the Gaussian03 package. Also, the ChelpG [33] charges were calculated at the B3LYP/6-311++G(d,p) level of theory to investigate the charge transfer between two units. Cube files containing the MEP information have been generated for complexes at the B3LYP/6-311++G(d,p) level of theory. The freely available MOLEKEL program [34] has been used for the visualization of the MEP data. The most negative-valued MEP point ($V_{\min}$) can be obtained from visual inspection of MEP data for the lone-pair region of the nitrogen atoms in pyridazine. The B3LYP-optimized geometries with the 6-311++G(d,p) basis set were then used to perform interaction energy decomposition using the SAPT scheme. Molecular integrals were first obtained with the GAMESS package [35], and the SAPT partitioning was performed using the SAPT-2008 program [36].

3. Results and Discussion

The most important geometrical parameters of complexes optimized at the B3LYP/6-311++G(d,p) level of theory are gathered in Table 1. The maximum and minimum values of the N$\cdots$H bond length correspond to NO_2 and $N(CH_3)_2$ substituents, respectively, in all cases. Also, the N$\cdots$H bond length in the complex **1** is longer than that in the complexes **2** and **3**. On the other hand, the N$\cdots$H bond length in the complex **2** is longer than that in the complex **3**. These results show that the cooperativity of H-bond interactions leads to the elongation of the N$\cdots$H bond lengths.

The total binding energies of complexes (ΔE) calculated at the B3LYP/6-311++G(d,p) level of theory and corrected for BSSE are summarized in Table 2. The results show that the stabilization energies of the complex **3** are larger than those of complex **2**. As can be seen, the maximum and minimum values of ΔE calculated at the B3LYP/6-311++G(d,p) level of theory correspond to the $N(CH_3)_2$ and NO_2 substituents, respectively.

The results of single-point energy calculation at the MP2/6-311++G (d,p), MP2/aug-cc-pVDZ, PBE1KCIS/6-311++G(d,p), and PBE1KCIS/aug-cc-pVDZ levels of theory on the geometries optimized at the B3LYP/6-311++G(d,p) level of theory are also given in Table 2. The maximum and minimum ΔE values correspond to $N(CH_3)_2$ and NO_2 substituents, respectively, at all levels of theory.

The ΔE values calculated by the MP2 method increase by 13.8 to 7.6 percent going from 6-311++G(d,p) to aug-cc-pVDZ basis sets. The corresponding changes are in the range of -0.51 to -0.19 kcal mol^{-1} for the values calculated by the PBE1KCIS method.

The absolute values of ΔE calculated at the MP2/6-311++G(d,p) level are 2.07 to 4.22 kcal mol^{-1} smaller than those calculated at the B3LYP/6-311++G(d,p) level. The absolute values of ΔE calculated by the PBE1KCIS method are approximately 3.54 to 0.51 kcal mol^{-1} larger than the values calculated by the MP2 and B3LYP methods. The ΔE values calculated at the PBE1KCIS/aug-cc-pVDZ level are approximately identical with the values calculated at the B3LYP/6-311++G(d,p) level of theory.

The BSSE-corrected binding energies of the complex **1** are lower than the sum of binding energies of the complexes **2** and **3** (see Table 2). In addition, the stabilization energies of complexes become more negative by the electron-donating substituents (with the exception of the OH substituent in the complex **2**) relative to the pyridazine, while the behavior is reversed by the electron-withdrawing substituents.

The total substituent effect comprises inductive/field effects, which have electrostatic character, and resonance effects, which are not electrostatic in nature. Resonance effects are strongest at para position, while the electrostatic interactions inversely depend on distance [38, 39]. The Hammett substituent constants are presented in Table 1 [37]. For the $N(CH_3)_2$, $NHCH_3$, NH_2, CH_3, and C_2H_5 substituents, the σ_p values are more negative than the σ_m values, so, the electron donation of the aforementioned substituents in the complex **3** is higher than that in the complex **2**. The high

Table 1: The N· · · H bond lengths optimized at the B3LYP/6-311++G(d,p) level in (Å) and the Hammett constants.

	Bond length			Hammett constants				
	Complex **1**	Complex **2**	Complex **3**	σ_m	σ_p	σ_{total}	σ_I	σ_R
$N(CH_3)_2$	1.67 (1.69)	1.64	1.63	−0.15	−0.83	−0.98	0.15	−0.98
$NHCH_3$	1.68 (1.70)	1.65	1.63	−0.52	−0.74	−1.26	0.03	−0.73
NH_2	1.68 (1.71)	1.65	1.64	−0.16	−0.66	−0.82	0.08	−0.74
CH_3	1.71 (1.71)	1.66	1.66	−0.07	−0.17	−0.24	0.01	−0.18
C_2H_5	1.71 (1.71)	1.66	1.66	−0.07	−0.15	−0.22	0.00	−0.15
OCH_3	1.70 (1.72)	1.67	1.65	0.12	−0.27	−0.15	0.29	−0.56
OH	1.71 (1.73)	1.67	1.66	0.12	−0.37	−0.25	0.30	−0.70
H	1.72 (1.72)	1.67	1.67	0.00	0.00	0.00		
OF	1.73 (1.74)	1.70	1.68	0.47	0.36	0.83		
CN	1.75 (1.70)	1.71	1.70	0.56	0.66	1.22	0.51	0.15
NO_2	1.76 (1.76)	1.72	1.71	0.71	0.78	1.49	0.60	0.13
F	1.73 (1.74)	1.69	1.68	0.34	0.06	0.40	0.45	−0.39
Br	1.73 (1.74)	1.69	1.69	0.39	0.23	0.62	0.40	−0.22
Cl	1.73 (1.74)	1.69	1.68	0.37	0.23	0.60	0.42	−0.19

The data in the parentheses correspond to the $N_2 \cdots H$ bond length. The σ values are taken from [37].

Table 2: The binding energies ($-\Delta E$ in kcal mol^{-1}) corrected for BSSE calculated at different levels.

	Complex **1**			Complex **2**			Complex **3**		
	B3LYP	MP2	PBE1KCIS	B3LYP	MP2	PBE1KCIS	B3LYP	MP2	PBE1KCIS
$N(CH_3)_2$	25.75	21.90 (23.52)	26.22 (25.86)	13.92	11.90 (12.81)	14.19 (14.03)	14.48	11.72 (12.70)	14.71 (14.49)
$NHCH_3$	25.32	21.80 (23.23)	25.81 (25.42)	13.73	12.00 (12.74)	13.99 (13.82)	14.31	11.82 (12.60)	14.54 (14.31)
NH_2	24.51	20.30 (22.12)	25.06 (24.66)	13.27	11.30 (12.14)	13.55 (13.38)	13.88	11.14 (12.10)	14.15 (13.91)
CH_3	22.98	19.80 (21.10)	23.44 (23.07)	12.80	10.90 (11.63)	13.03 (12.85)	12.86	10.82 (11.50)	13.08 (12.88)
C_2H_5	23.34	19.80 (21.44)	23.88 (23.64)	13.01	10.90 (11.86)	13.32 (13.24)	13.09	10.78 (11.80)	13.40 (13.31)
OCH_3	23.19	19.90 (21.24)	23.65 (23.31)	12.61	10.90 (11.55)	12.85 (12.68)	13.20	10.99 (11.70)	13.43 (13.24)
OH	22.42	19.30 (20.69)	22.96 (22.67)	12.29	10.60 (11.34)	12.57 (12.43)	12.72	10.61 (11.30)	12.98 (12.81)
H	22.01	19.00 (20.28)	22.45 (22.07)	12.33	10.50 (11.17)	12.55 (12.35)	12.33	10.50 (11.20)	12.55 (12.35)
OF	20.10	17.60 (18.89)	20.70 (20.56)	10.99	9.59 (10.29)	11.29 (11.21)	11.56	9.82 (10.50)	11.86 (11.76)
CN	18.33	16.00 (17.10)	18.76 (18.42)	10.21	8.66 (9.26)	10.41 (10.22)	10.43	9.03 (9.62)	10.64 (10.46)
NO_2	17.59	15.50 (16.74)	18.14 (17.95)	9.85	8.40 (9.04)	10.10 (9.99)	10.03	8.88 (9.50)	10.30 (10.19)
F	20.30	17.60 (18.86)	20.84 (20.57)	11.20	9.65 (10.28)	11.46 (11.31)	11.63	9.86 (10.50)	11.89 (11.75)
Br	20.28	17.70 (18.86)	20.79 (20.42)	11.16	9.63 (10.23)	11.41 (11.23)	11.51	9.89 (10.50)	11.75 (11.58)
Cl	20.29	17.70 (18.81)	20.80 (20.44)	11.18	9.65 (10.22)	11.43 (11.24)	11.55	9.91 (10.50)	11.80 (11.61)

The data in the parenthesis correspond to the aug-cc-pVDZ basis set.

electronegativity of oxygen makes the OCH_3 and OH substituents electron-withdrawing by the inductive effect; this is reflected in the positive value for σ_m.

Recall that the meta substituents only affect the reaction center by the inductive effects, whereas the para substituents affect it by both the inductive and resonance effects. Thus, there is a satisfactory linear relationship between ΔE and $\sigma_I (R = 0.91)$, ΔE and $\sigma_I + \sigma_R (R = 0.98)$, respectively, in the complexes **2** and **3**. Comparing the σ values for the meta and para indicates that the electron-donating resonance effect (σ_R) dominates over the electron-withdrawing inductive effect (σ_I). Therefore, these substituents are more electron-donating in the complex **3** in comparison to the complex **2**. The σ_m and σ_p values are positive for the OF, CN, NO_2, F, Br, and Cl substituents. Thus, these substituents are electron-withdrawing in both the meta and para positions. Comparison between the σ values for the meta and para indicates that the σ_I dominates over the σ_R. Since the inductive effect is inversely related to distance, the electron-withdrawing inductive effects are stronger in the complex **2** in comparison with the complex **3**.

The σ_m and σ_p constants can be used as appropriate parameters for the description of the intermolecular interaction in the X-pyridazine· · · $(HF)_2$ complex. The linear correlation coefficient between the ΔE values and the σ_m, σ_p, and $\sigma_{\text{total}}(\sigma_m + \sigma_p)$ constants is equal to 0.95, 0.97, and 0.98, respectively. This indicates that the total electrostatic effect of the substituents as well as induction and resonance vitally impacts the two intermolecular interactions (see Figure 1).

3.1. AIM and NBO Analysis. A way to characterize the hydrogen bond is AIM analysis that interprets these interactions in terms of critical points [40, 41]. The values of electron density (ρ) calculated at the $N_2 \cdots H$ and $N_1 \cdots H$ bond critical points (BCPs) of complexes **1–3** are gathered in Table 3.

Table 3: Electron densities ρ (in e/au^3) at the N$\cdots$H BCP in the X-pyridazine$\cdots$(HF)$_n$(n = 1, 2) complexes and individual H-bond energies E (in kcal mol^{-1}) calculated for the complex **1**.

	Complex **1**		Complex **2**	Complex **3**
	$\rho_{BCP} \times 10^2$	E	$\rho_{BCP} \times 10^2$	$\rho_{BCP} \times 10^2$
$N(CH_3)_2$	**5.46**, *5.23*	**−14.41**, *−13.44*	6.03	6.16
$NHCH_3$	**5.40**, *5.15*	**−14.23**, *−13.18*	5.95	5.95
NH_2	**5.32**, *5.05*	**−13.85**, *−12.73*	5.82	5.97
CH_3	**4.99**, *4.95*	**−12.36**, *−12.21*	5.69	5.69
C_2H_5	**5.02**, *5.00*	**−12.76**, *−12.67*	5.73	5.74
OCH_3	**5.08**, *4.91*	**−12.98**, *−12.29*	5.60	5.79
OH	**5.02**, *4.79*	**−12.66**, *−11.75*	5.56	5.65
H	**4.83**, *4.83*	**−12.04**, *−12.04*	5.54	5.54
OF	**4.70**, *4.55*	**−11.37**, *−10.81*	5.19	5.35
CN	**4.45**, *4.43*	**−10.22**, *−10.15*	5.01	5.07
NO_2	**4.42**, *4.45*	**−10.08**, *−10.19*	4.90	4.90
F	**4.71**, *4.57*	**−11.46**, *−10.92*	5.23	5.36
Br	**4.69**, *4.61*	**−11.33**, *−11.02*	5.24	5.33
Cl	**4.69**, *4.60*	**−11.36**, *−11.02*	5.25	5.35

The bold and italicized values correspond to the N$_1\cdots$H and N$_2\cdots$H hydrogen bonds, respectively.

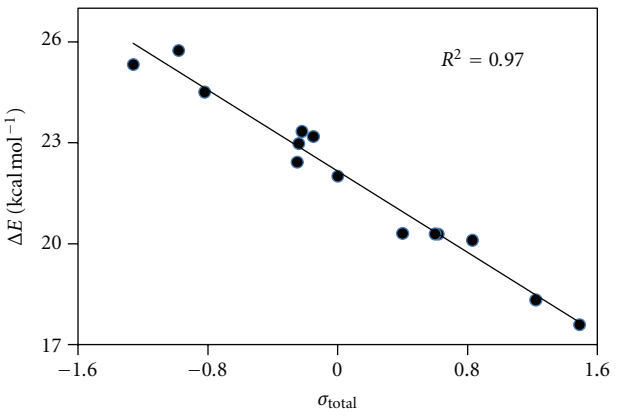

Figure 1: Correlation between the binding energies ($-\Delta E$ in kcal mol^{-1}) and Hammett constant σ_{total} for the complex **1**.

The maximum and minimum values correspond to the $N(CH_3)_2$ and NO_2 substituents, respectively, (with the exception of ρ_{N_2H} in the complex **1** where the minimum value corresponds to the CN substituent). The topological properties of ρ calculated at the BCP of the intermolecular hydrogen bonds may be treated as a measure of the hydrogen bond strength [42–44]. The electron-withdrawing substituents pull the lone pair of nitrogen atoms of pyridazine inside the ring and decrease the ρ values at the N$\cdots$H BCP, while the electron-donating substituents increase the ρ values and enhance the hydrogen bond strength. The ρ values calculated at the N$\cdots$H BCP in the complex **3** are higher than those in the complex **2**, and the complex **3** is more stable than the complex **2**. On the other hand, the ρ values of N$\cdots$H hydrogen bond of complex **1** are lower than the values calculated at the N$_2\cdots$H and N$_1\cdots$H hydrogen bonds in the complexes **2** and **3**. Thus, a negative cooperativity is predicted from the comparison between $\rho_{N\cdots H}$ values in the complex **1** and the complexes **2** and **3**. The N$\cdots$H bond length decreases linearly by the increase in the ρ values calculated at the N$\cdots$H BCP for all categories ($R^2 \simeq 0.99$). Also, there is a linear relationship between ρ and ΔE for all cases. A linear relationship ($R^2 = 0.99$) is observed between the ΔE values calculated at the B3LYP/6-311++G(d,p) level and the ρ values calculated at the N$\cdots$H BCPs in the complex **1**.

Because of linear relationship between ΔE and ρ_{NH} values, the $\Delta E = c\rho_{NH}$ can be used for the calculation of individual H-bond energies in the complex **1** (see Table 4). All individual H-bond energies calculated for the complex **1** are lower than the values calculated for the complexes **2** and **3**. Also, there is a linear relationship with high correlation coefficient ($R = 0.99$) between individual H-bond energies and the N$\cdots$H bond lengths.

For a better understanding of the hydrogen bond interaction in the complexes **1–3**, the NBO analysis has been carried out at the HF/6-311++G(d,p) level of theory. The $lp_N \rightarrow \sigma^*_{HF}$ interaction, which can be considered as a measure of charge transfer, has been evaluated in the complexes **1–3** (see Table 5). The donor-acceptor interaction energy (E^2) value of this interaction can be used to predict the strength of the N$\cdots$H hydrogen bond. In all cases, the maximum and minimum values correspond to the $N(CH_3)_2$ and NO_2 substituents, respectively. As can be seen in Table 4, the E^2 values of the $lp_{N_2} \rightarrow \sigma^*_{HF}$ and $lp_{N_1} \rightarrow \sigma^*_{HF}$ interactions in the complexes **2** and **3** are higher than those in the complex **1**. So, the negative cooperativity decreases the E^2 values of $lp_{N_2} \rightarrow \sigma^*_{HF}$ and $lp_{N_1} \rightarrow \sigma^*_{HF}$ donor-acceptor interactions in the complex **1** relative to the complexes **2** and **3**. The electron-donating substituents increase the electron density on the nitrogen atoms of pyridazine ring (with the exception of OH substituent in the complex **2**) and increase their inclination on polarization of HF, which increase the E^2 value of the $lp_N \rightarrow \sigma^*_{HF}$ interaction. Though OH is an electron-donating substituent, but it destabilizes the complex **2** relative to the pyridazine. This behavior is not observed for the OCH_3 functional group. The NBO atomic charge on the O (−0.71) of OH substituent is more negative than O (−0.61) of the OCH_3 substituent. Thus, electron-withdrawing induction effect is predominant over the electron-donating resonance effect by the high electronegativity of O atom in the OH substituent. Moreover, there are good linear relationships between the E^2 values and both the σ_{total} values and N$\cdots$H bond lengths.

The occupation numbers of lp_{N_2}, lp_{N_1}, and σ^*_{HF} are given in Table 4. The maximum and minimum occupancies for lp_{N_2} and lp_{N_1} correspond to NO_2 and $N(CH_3)_2$, respectively, the maximum and minimum occupancies of σ^*_{HF} correspond to $N(CH_3)_2$ and NO_2, respectively. As can be seen in Table 4, increasing the occupation numbers of lp_{N_2} and lp_{N_1} is accompanied with the decrease in the occupation number of σ^*_{HF} for all complexes. The occupancies of lp_{N_2} and lp_{N_1} in the complex **1** are larger than those in the complexes **2** and **3**, while the occupancy of σ^*_{HF} in the complexes **2** and **3** is larger than that in the complex **1**. Thus, the occupancy of the first lp_N/σ^*_{HF} increases/decreases in the presence of second

Table 4: The results of NBO analysis for the X-pyridazine$\cdots$(HF)$_n$ ($n = 1, 2$) complexes at the HF/6-311++G(d,p) level of theory.

	Complex **1**			Complex **2**			Complex **3**		
	E^2	lp_N	σ^*_{HF} ($\times 10^2$)	E^2	lp_N	σ^*_{HF} ($\times 10^2$)	E^2	lp_N	σ^*_{HF} ($\times 10^2$)
$N(CH_3)_2$	**34.16**, *30.47*	**1.911**, *1.914*	**4.509**, *5.030*	39.48	1.904	5.767	42.41	1.902	6.166
$NHCH_3$	**33.46**, *29.71*	**1.912**, *1.915*	**4.395**, *4.934*	38.66	1.906	5.651	41.79	1.903	6.087
NH_2	**32.52**, *28.72*	**1.913**, *1.917*	**4.236**, *4.793*	37.35	1.908	5.438	40.05	1.905	5.838
CH_3	**28.59**, *27.95*	**1.919**, *1.920*	**4.148**, *4.239*	36.07	1.911	5.289	36.44	1.910	5.333
C_2H_5	**28.94**, *28.42*	**1.919**, *1.919*	**4.213**, *4.288*	36.62	1.910	5.394	36.91	1.910	5.399
OCH_3	**29.60**, *27.51*	**1.917**, *1.920*	**5.604**, *5.946*	35.08	1.912	5.101	37.70	1.900	5.503
OH	**29.01**, *25.99*	**1.918**, *1.921*	**3.859**, *4.286*	34.39	1.912	5.031	36.12	1.910	5.273
H	**26.79**, *26.73*	**1.921**, *1.921*	**3.982**, *3.982*	34.69	1.912	5.093	34.69	1.912	5.093
OF	**25.44**, *23.61*	**1.922**, *1.924*	**4.931**, *5.238*	30.95	1.918	4.520	32.49	1.915	4.760
CN	**22.58**, *22.52*	**1.928**, *1.926*	**3.348**, *3.352*	28.57	1.919	4.200	29.04	1.921	4.259
NO_2	**21.48**, *21.68*	**1.929**, *1.928*	**4.566**, *4.556*	27.26	1.922	3.993	27.64	1.922	4.041
F	**25.50**, *23.92*	**1.922**, *1.925*	**3.533**, *3.785*	30.95	1.918	4.520	32.63	1.914	4.774
Br	**25.29**, *24.36*	**1.923**, *1.923*	**3.622**, *3.757*	31.14	1.915	4.575	32.23	1.916	4.723
Cl	**25.36**, *24.28*	**1.923**, *1.923*	**3.602**, *3.763*	31.16	1.916	4.570	32.40	1.915	4.745

The E^2 values are in kcal mol^{-1}. The bold and italicized values correspond to the $N_1 \cdots H$ and $N_2 \cdots H$ bonds, respectively.

Table 5: The results of MEP analysis ($V_{min} \times 10^3$) and charge transfer ($\Delta q \times 10^3$ in au) calculated from ChelpG charges.

	Complex **1**		Complex **2**		Complex **3**	
	V_{min}	Δq	V_{min}	Δq	V_{min}	Δq
$N(CH_3)_2$	97	**205**, *194*	103	295	107	309
$NHCH_3$	96	**199**, *187*	101	282	106	293
NH_2	94	**193**, *189*	99	283	103	294
CH_3	87	**189**, *195*	96	294	97	291
C_2H_5	88	**190**, *200*	97	292	98	296
OCH_3	89	**181**, *204*	98	288	99	295
OH	86	**192**, *188*	92	293	96	295
H	84	**194**, *195*	94	300	94	300
OF	79	**182**, *182*	88	278	89	280
CN	73	**175**, *185*	83	277	82	279
NO_2	72	**178**, *182*	81	278	80	270
F	79	**186**, *181*	88	280	89	279
Br	80	**213**, *163*	89	325	90	328
Cl	80	**189**, *176*	89	275	90	285

The bold and italicized values correspond to the charge transfer from N_1 and N_2 atoms to HF unit, respectively.

$N\cdots HF$ interaction. This confirms the negative cooperativity in the complex **1**. There is a little difference between the occupancies of lp_{N_2} and lp_{N_1} in the complexes **2** and **3**. Also, the occupancy of σ^*_{HF} in the complex **3** is larger than that in the complex **2**. Therefore, the changes of occupation numbers of lp_{N_2}, lp_{N_1}, and σ^*_{HF} are in agreement with the binding energies in all categories. A linear relationship ($R^2 = 1.0$) is observed between the ΔE values and the sum of E^2 values of $lp_{N_1} \rightarrow \sigma^*_{HF}$ and $lp_{N_1} \rightarrow \sigma^*_{HF}$ in the complex **1**. The high linear correlation ($R^2 = 1.0$) indicates the additivity of the E^2 values of two H-bond interactions.

There is also a linear relationship between the E^2 values and the occupancies of lp_{N_2}, lp_{N_1}, and σ^*_{HF}. In addition, there is a linear relationship between E^2 and $N\cdots H$ hydrogen bond lengths in three categories. Linear relationships are observed for the E^2 value of $lp_{N_2} \rightarrow \sigma^*_{HF}$ versus $r_{N_2\cdots H}$ ($R^2 = 0.98$) and the E^2 values of $lp_{N_1} \rightarrow \sigma^*_{HF}$ versus $r_{N_1\cdots H}$ ($R^2 = 0.99$) in the complex 1.

On the base of charges calculated by the ChelpG method (see Table 5), the charge transfer occurred from X-pyridazine to HF unit, The electron-donating substituents promote the charge transfer from X-pyridazine to HF unit, and enhance the basicity of the nitrogen atoms in the X-pyridazine. In the complex **3**, the charge transfer is larger and the basicity of N atom is higher than those in the complex **2**; this can be a reason for the stability of complex **3**. On the other hand, the charge transfer in the complex **1** is lower than that in complexes **2** and **3**; this is in agreement with the negative cooperativity of two hydrogen bond interactions.

3.2. MEP Analysis. The MEP is an important tool in exploring the nature of intermolecular interactions [45–51]. The capability of the N_2 and N_1 atoms to accept hydrogen bond was estimated through the minimum of the MEP (V_{min}) around the nitrogen atoms. As can be seen in Table 5, the MEP values become more negative with the electron-donating substituents. Thus, the electrostatic term depends on the electron donation or electron withdrawal character of the substituents. Also, a good linear relationship is observed between the V_{min} values and the σ_{total} values (see Figure 2). Therefore, those values can be used to predict the Hammett constants. The trend in the V_{min} values is **3** > **2** > **1**; so, those values become less negative around the nitrogen atoms when both interactions coexist.

The MEP, $V_{(r)}$, is directly related to electron density $\rho(r)$ through the Poisson's equation [52]:

$$\nabla^2 V(r) = 4\pi\rho(r). \quad (1)$$

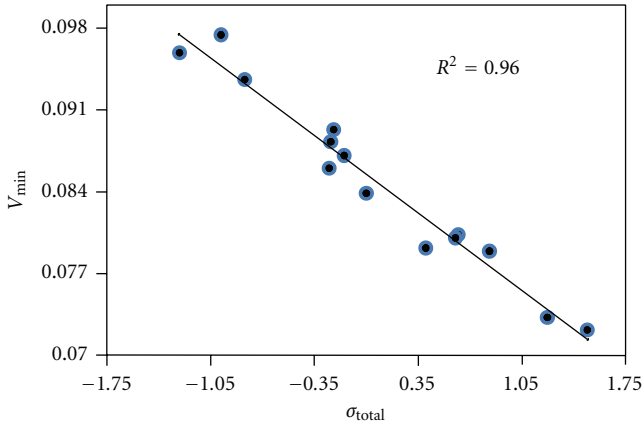

FIGURE 2: Linear correlation between molecular electrostatic potential minimum (V_{min}) around the nitrogen atoms of the pyridazine and the Hammett electronic parameters for the complex **1**.

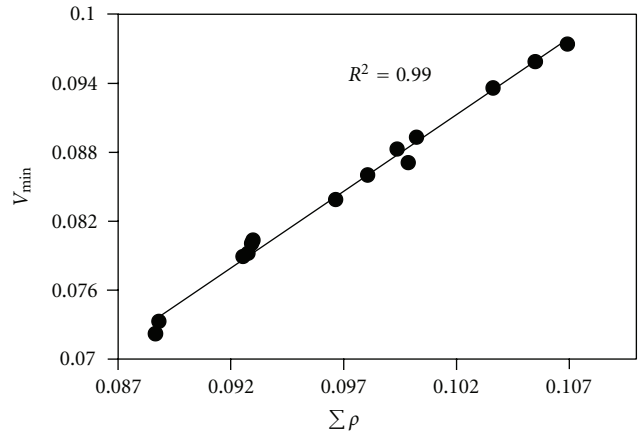

FIGURE 3: Interplay between the V_{min} value around the nitrogen of pyridazine versus the sum of ρ values calculated at the N$\cdots$H BCPs for complex **1**.

Is there a liner relationship between V_{min} and the ρ values calculated at the HBCPs? The V_{min} values become more negative with increasing ρ values calculated at HBCPs in X-pyridazine$\cdots$(HF)$_n$ complexes. The linear correlation coefficients between the V_{min} values and the ρ values are equal to 0.98 and 0.99, respectively, in the complexes **2** and **3**. As can be seen in Figure 3, there is a good correlation between V_{min} values and $\sum\rho$ values for the complex **1** ($R = 1.00$). Similarly, there is a linear relationship ($R = 0.99$) between V_{min} and E^2 of $lp_N \rightarrow \sigma^*_{HF}$ interaction, V_{min}, and the $N_2\cdots H$ and $N_1\cdots H$ bond lengths. Also, there is a good linear correlation between V_{min} values and $\sum E^2$ in the complex **1** ($R = 1.00$).

3.3. SAPT Energy Decomposition. The SAPT analysis is a method for investigation the nature of the intermolecular interactions [53–55]. The SAPT method provides detailed information on the intermolecular interaction, as this method directly calculates magnitude of each term (electrostatic, dispersion, etc.) of the intermolecular interactions [56]. A detailed description of SAPT and some of its applications can be found in some recent references [57–59].

To determine the nature of the hydrogen bond in the complexes **2** and **3**, the interaction energies were decomposed into physically meaningful components, including electrostatic, induction, dispersion, and exchange energies, using SAPT technique at the B3LYP/6-31G(d) level. It can be seen from Table 6 that the values of electrostatic energy (E_{els}), induction energy (E_{ind}), and dispersion energy (E_{disp}) are negative, whereas the exchange energy (E_{exch}) is positive for all complexes. Thus, the stabilization/destabilization of the complexes by substitution is represented simply by the sum from E_{els}, E_{ind}, and E_{disp} contributions. In both complexes, the absolute values for these three negative terms are largest for the $N(CH_3)_2$ substituent and are smallest for the NO_2 substituent. In the complex **3**, the absolute values of E_{els}, E_{ind}, and E_{disp} are larger than those values in the complex **2**. Thus, the complex **3** is more stable than the complex **2**. The electron-donating substituents have positive effect and increase the magnitude of the calculated SAPT interaction energy components (with the exception of OH substituent in the complex **2** that decreases the magnitude of electrostatic energy relative to pyridazine). The electron-withdrawing substituents have negative effect and decrease the magnitude of interaction energy components, with the exception of E_{disp} in the complex **2** that slightly increases in the presence of mentioned substituents. The dependence of the dispersion term to the substituent is smaller than other complexes. When position of HF changes from para to meta relative to the substituent, the electrostatic term changes by 2.8%, the induction term changes by 2.2%, and the dispersion term changes by 12.5%. Thus, the dispersion energy component of the SAPT analysis was found to be very sensitive to the position of HF relative to the substituent.

In the complex **2**, the electrostatic forces contribute about 52.0–54.6% to the total attractive interaction energy, the induction forces are about 35.6–43.6% of the total attractive energy, and the dispersion contribution is 9.7–11.9%. On the other hand, the electrostatic, induction, and dispersion contributions are 51.9–52.6%, 36.4–37.0%, and 10.5–11.7%, respectively, in the complex **3**. Thus, we believe that the electrostatic interactions are mainly responsible for the binding energies and formation of hydrogen bonds, although the induction and dispersion interactions are also important. Since the electrostatic plays an important role, the polarization correlates with the electrostatic energy. The electron-withdrawing substituents hinder the electron transfer-driven polarization to the HF unit (which results in destabilization), whereas the electron-donating substituents allow strong polarization to the HF unit (which results in strong stabilization). It is also interesting to note that the polarization for the electron-donating and electron-withdrawing substituents in the complex **2** is slightly weaker than that in the complex **3**. In the complex **3**, the electron density at the para position is an important stabilizing factor, and thus the stabilization/destabilization by substituent of a pyridazine is governed mostly by the electrostatic energy. In Figure 4, a linear

Table 6: SAPT interaction energy decomposition (in kcal mol^{-1}) for the complexes **2** and **3**.

	Complex **2**					Complex **3**				
	E_{els}	E_{ind}	E_{exch}	E_{disp}	E_{int}^{SAPT}	E_{els}	E_{ind}	E_{exch}	E_{disp}	E_{int}^{SAPT}
$N(CH_3)_2$	−25.53	−17.74	34.24	−5.16	−14.18	−26.21	−18.48	35.29	−5.27	−14.67
$NHCH_3$	−25.15	−17.41	33.69	−5.08	−13.94	−25.93	−18.29	35.00	−5.22	−14.45
NH_2	−24.34	−16.81	32.71	−4.95	−13.39	−25.16	−17.66	33.94	−5.09	−13.97
CH_3	−23.5	−16.35	31.87	−4.84	−12.83	−23.51	−16.40	31.90	−4.84	−12.84
C_2H_5	−23.73	−16.53	32.16	−4.88	−12.98	−23.75	−16.59	32.23	−4.88	−13.00
OCH_3	−22.95	−15.86	31.01	−4.75	−12.55	−23.99	−16.83	32.64	−4.94	−13.11
OH	−22.62	−15.72	30.90	−4.74	−12.19	−23.08	−16.16	31.54	−4.80	−12.51
H	−22.80	−14.89	29.63	−4.06	−12.12	−22.70	−15.73	30.81	−4.69	−12.31
OF	−20.06	−14.07	27.96	−4.41	−10.59	−21.04	−14.78	29.27	−4.54	−11.09
CN	−18.92	−13.48	26.85	−4.28	−9.84	−19.37	−13.65	27.22	−4.31	−10.11
NO_2	−18.05	−12.92	25.87	−4.17	−9.28	−18.64	−13.06	26.27	−4.20	−9.62
F	−20.35	−14.27	28.35	−4.43	−10.71	−21.13	−14.84	29.39	−4.54	−11.12
Cl	−20.52	−14.49	28.57	−4.48	−10.93	−21.13	−14.84	29.29	−4.55	−11.23

All energies are in kcal mol^{-1}. $E_{int}^{SAPT} = E_{els} + E_{ind} + E_{disp} + E_{exch}$.

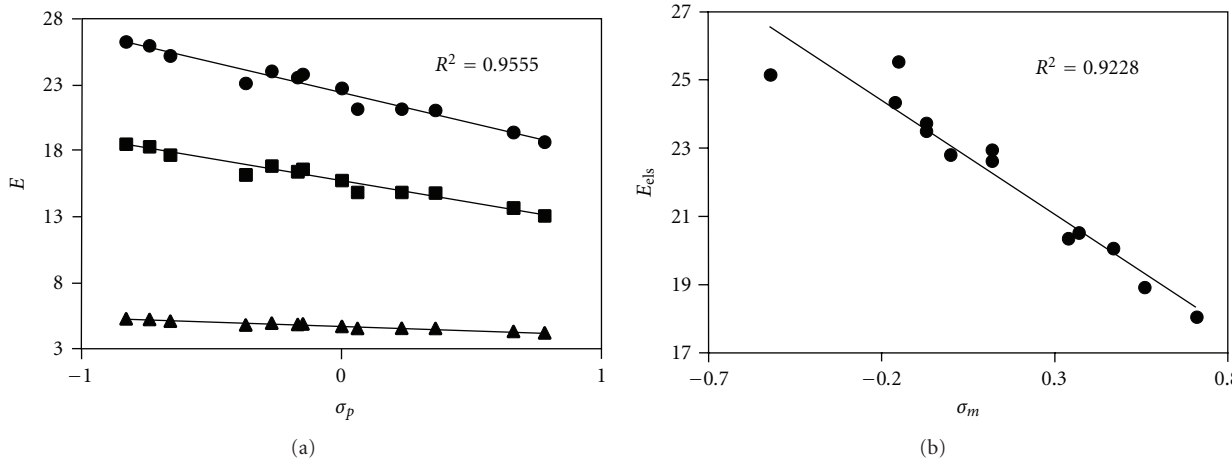

Figure 4: Linear relationship between the calculated SAPT interaction energy components (•E_{els}, ■E_{ind}, and ▲E_{dis} in kcal mol^{-1}) and σ_p for the complex **3** (a), and the electrostatic energy and σ_m for the complex **2** (b).

relationship with high correlation coefficient ($R = 0.98$) is observed between the calculated SAPT interaction energy components and σ_p in the complex **3**. In the complex **2**, a linear relationship with correlation coefficient 0.96 is found between the E_{els} and σ_m.

4. Conclusions

The results of quantum mechanical calculations indicate that the binding energy in the complex **3** is larger than that in the complex **2**. The sum of binding energies of the complexes **2** and **3** is larger than the binding energy of the complex **1**. So, there is a negative cooperativity for two hydrogen bond interactions.

Very good linear correlations are observed between the binding energies and Hammett electronic parameters σ_{total} of the substituents. The electron-donating substituents stabilize and the electron-withdrawing substituents destabilize the complexes relative to pyridazine. According to the results of AIM analysis, the cooperativity effect decreases the electron density at the N$\cdots$H BCPs in the X-pyridazine$\cdots$(HF)$_2$ complex.

On the basis of the results of SAPT analysis, the portion of electrostatic force in the complex **3** is smaller than **2**, while the induction and dispersion portions are larger in the complex **3**. The E^2 values of $lp_{N_2} \rightarrow \sigma^*_{HF}$ and $lp_{N_1} \rightarrow \sigma^*_{HF}$ interactions in the complex **1** are smaller than those in the complexes **2** and **3**. Thus, the cooperativity effect decreases the E^2 values of $lp_{N_2} \rightarrow \sigma^*_{HF}$ and $lp_{N_1} \rightarrow \sigma^*_{HF}$ interactions in the complex **1**. The occupation numbers of lp_{N_2} and lp_{N_1} in the complex **1** are larger than those in the complexes **2** and **3**, respectively. The charge transfer, on the basis of ChelpG charges, is in agreement with the results of NBO and AIM analysis.

There are linear relationships between the V_{min} and ρ_{BCP} values, the V_{min} and the E^2 values of $lp_N \rightarrow \sigma^*_{HF}$ interaction, and between the V_{min} and the σ_{total} values.

The SAPT calculations show that the electrostatic is the dominating interaction component in the complexes **2** and **3**, although the induction and dispersion interactions are also important. The dispersion energy component of the SAPT analysis was found to be very sensitive to the position of HF relative to the substituent. There is a good correlation between σ_p and the calculated SAPT interaction energy components in the complex **3**, while the linear relationship is only found between the E_{els} and σ_m in the complex **2**.

References

[1] S. Breda, I. D. Reva, L. Lapinski, M. J. Nowak, and R. Fausto, "Infrared spectra of pyrazine, pyrimidine and pyridazine in solid argon," *Journal of Molecular Structure*, vol. 786, no. 2-3, pp. 193–206, 2006.

[2] X. J. Zou, G. Y. Jin, and Z. X. Zhang, "Synthesis, fungicidal activity, and QSAR of pyridazinonethiadiazoles," *Journal of Agricultural and Food Chemistry*, vol. 50, no. 6, pp. 1451–1454, 2002.

[3] S. G. Lee, J. J. Kim, H. K. Kim et al., "Recent progress in pyridazin-3(2H)-ones chemistry," *Current Organic Chemistry*, vol. 8, no. 15, pp. 1463–1480, 2004.

[4] R. V. A. Orru and M. de Greef, "Recent advances in solution-phase multicomponent methodology for the synthesis of heterocyclic compounds," *Synthesis*, no. 10, pp. 1471–1499, 2003.

[5] N. G. Kandile, M. I. Mohamed, H. Zaky, and H. M. Mohamed, "Novel pyridazine derivatives: synthesis and antimicrobial activity evaluation," *European Journal of Medicinal Chemistry*, vol. 44, no. 5, pp. 1989–1996, 2009.

[6] G. R. Desiraju and T. Steiner, *The Weak Hydrogen Bond in Structural Chemistry and Biology*, Oxford University Press, Oxford, UK, 1997.

[7] G. R. Desiraju and T. Steiner, *The Weak Hydrogen Bond*, Oxford University Press, Oxford, UK, 1999.

[8] M. Nishio, M. Hirota, and Y. Umezawa, *The CH/π Interaction*, Wiley-VCH, New York, NY, USA, 1998.

[9] S. Scheiner, Ed., *Molecular Interactions: from van der Waals to Strong Bound Complexes*, John Wiley & Sons, Chichester, UK, 1997.

[10] S. Scheiner, Ed., *Hydrogen Bonding: A Theoretical Perspective*, Oxford University Press, Oxford, UK, 1997.

[11] G. A. Jeffrey and W. Saenger, *Hydrogen Bonding in Biological Structures*, Springer, Berlin, Germany, 1991.

[12] G. A. Jeffrey, *An Introduction to Hydrogen Bonding*, Oxford University Press, Oxford, UK, 1997.

[13] W. Wang, Y. Zhang, and K. Huang, "Unconventional interaction in N(P)-related systems," *Chemical Physics Letters*, vol. 411, no. 4–6, pp. 439–444, 2005.

[14] W. Chen and M. S. Gordon, "Energy decomposition analyses for many-body interaction and applications to water complexes," *Journal of Physical Chemistry*, vol. 100, no. 34, pp. 14316–14328, 1996.

[15] A. D. Kulkarni, R. K. Pathak, and L. J. Bartolotti, "Effect of additional hydrogen peroxide to $H_2O_2 \cdots (H_2O)n$, $n = 1$ and 2 complexes: quantum chemical study," *Journal of Chemical Physics*, vol. 124, no. 21, Article ID 214309, 7 pages, 2006.

[16] Q. Li, X. An, F. Luan et al., "Cooperativity between two types of hydrogen bond in H_3 C-HCN-HCN and H_3 C-HNC-HNC complexes," *Journal of Chemical Physics*, vol. 128, no. 15, Article ID 154102, 6 pages, 2008.

[17] Y. L. Zhao and Y. D. Wu, "A theoretical study of β-sheet models: is the formation of hydrogen-bond networks cooperative?" *Journal of the American Chemical Society*, vol. 124, no. 8, pp. 1570–1571, 2002.

[18] R. Wieczorek and J. J. Dannenberg, "H-bonding cooperativity and energetics of α-helix formation of five 17-amino acid peptides," *Journal of the American Chemical Society*, vol. 125, no. 27, pp. 8124–8129, 2003.

[19] Q. Li, X. An, B. Gong, and J. Cheng, "Cooperativity between OH$\cdots$O and CH$\cdots$O hydrogen bonds involving dimethyl sulfoxide-H_2O-H_2O complex," *Journal of Physical Chemistry A*, vol. 111, no. 40, pp. 10166–10169, 2007.

[20] H. Guo, N. Gresh, B. P. Roques, and D. R. Salahub, "Many-body effects in systems of peptide hydrogen-bonded networks and their contributions to ligand binding: a comparison of the performances of DFT and polarizable molecular mechanics," *Journal of Physical Chemistry B*, vol. 104, no. 41, pp. 9746–9754, 2000.

[21] R. Viswanathan, A. Asensio, and J. J. Dannenberg, "Cooperative hydrogen-bonding in models of antiparallel β-sheets," *Journal of Physical Chemistry A*, vol. 108, no. 42, pp. 9205–9212, 2004.

[22] F. H. Allen, J. A. K. Howard, V. J. Hoy, G. R. Desiraju, D. Shekhar Reddy, and C. C. Wilson, "First neutron diffraction analysis of an O-H$\cdots\pi$ hydrogen bond: 2-ethynyladamantan-2-ol," *Journal of the American Chemical Society*, vol. 118, no. 17, pp. 4081–4084, 1996.

[23] B. S. Hudson, D. A. Braden, D. G. Allis et al., "The crystalline enol of 1,3-cyclohexanedione and its complex with benzene: vibrational spectra, simulation of structure and dynamics and evidence for cooperative hydrogen bonding," *Journal of Physical Chemistry A*, vol. 108, no. 36, pp. 7356–7363, 2004.

[24] R. F. W. Bader, *Atoms in Molecules: A Quantum Theory*, Oxford University Press, Oxford, UK, 1990.

[25] A. E. Reed, L. A. Curtiss, and F. Weinhold, "Intermolecular interactions from a natural bond orbital, donor-acceptor viewpoint," *Chemical Reviews*, vol. 88, no. 6, pp. 899–926, 1988.

[26] B. Jeziorski, R. Moszynski, and K. Szalewicz, "Perturbation theory approach to intermolecular potential energy surfaces of van der waals complexes," *Chemical Reviews*, vol. 94, no. 7, pp. 1887–1930, 1994.

[27] A. D. Becke, "Density-functional thermochemistry. III. The role of exact exchange," *Journal of Chemical Physics*, vol. 98, no. 7, pp. 5648–5652, 1993.

[28] M. J. Frisch, G. W. Trucks, H. B. Schlegel et al., *Gaussian 03 (Revision B.03)*, Gaussian, Pittsburgh, Pa, USA, 2003.

[29] C. Møller and M. S. Plesset, "Note on an approximation treatment for many-electron systems," *Physical Review*, vol. 46, no. 7, pp. 618–622, 1934.

[30] Y. Zhao and D. G. Truhlar, "Benchmark databases for nonbonded interactions and their use to test density functional theory," *Journal of Chemical Theory and Computation*, vol. 1, no. 3, pp. 415–432, 2005.

[31] S. F. Boys and F. Bernardi, "Calculation of small molecular interactions by differences of separate total energies—some procedures with reduced errors," *Molecular Physics*, vol. 19, no. 4, pp. 553–566, 1970.

[32] F. B. König, J. Schönbohm, and D. Bayles, "AIM2000—A program to analyze and visualize atoms in molecules," *Journal of Computational Chemistry*, vol. 22, no. 5, pp. 545–559, 2001.

[33] C. M. Breneman and K. B. Wiberg, "Determining atom-centered monopoles from molecular electrostatic potentials. The need for high sampling density in formamide conformational analysis," *Journal of Computational Chemistry*, vol. 11, no. 3, pp. 361–373, 1990.

[34] P. Flukiger, H. P. Luthi, S. Portmann, and J. Weber, *Molekel 4.0*, Swiss Center for Scientific Computing, Manno, Switzerland, 2000.

[35] M. W. Schmidt, K. K. Baldridge, J. A. Boatz et al., "General atomic and molecular electronic structure system," *Journal of Computational Chemistry*, vol. 14, no. 11, pp. 1347–1363, 1993.

[36] R. Bukowski, W. Cencek, P. Jankowski et al., *An Ab Initio Program for Many-Body Symmetry-Adapted Perturbation Theory Calculations of Intermolecular Interaction Energies. Sequential and Parallel Versions*, University of Delaware, Newark, Del, USA; University of Warsaw, Warsaw, Poland, 2008.

[37] C. Hansch, A. Leo, and R. W. Taft, "A survey of hammett substituent constants and resonance and field parameters," *Chemical Reviews*, vol. 91, no. 2, pp. 165–195, 1991.

[38] L. P. Hammett, "Some relations between reaction rates and equilibrium constants," *Chemical Reviews*, vol. 17, no. 1, pp. 125–136, 1935.

[39] F. Cozzi, F. Ponzini, R. Annunziata, M. Cinquini, and J. S. Siegel, "Polar interactions between stacked π systems in fluorinated 1,8-diarylnaphthalenes: Importance of quadrupole moments in molecular recognition," *Angewandte Chemie*, vol. 34, no. 9, pp. 1019–1020, 1995.

[40] M. Alcamí, O. Mó, and M. Yáñez, "Modelling intrinsic basicities: the use of the electrostatic potentials and the atoms-in-molecules theory," *Theoretical and Computational Chemistry*, vol. 3, pp. 407–456, 1996.

[41] C. H. Suresh and S. R. Gadre, "Electrostatic potential minimum on aromatic ring as a measure of substituent constant," *Inorganic Chemistry*, vol. 111, no. 4, pp. 710–714, 2007.

[42] A. Ebrahimi, M. Habibi, and H. R. Masoodi, "Theoretical study of the influence of para- and meta-substituents on X-pyridine$\cdots$HF hydrogen bonding," *Chemical Physics*, vol. 340, no. 1–3, pp. 85–92, 2007.

[43] S. J. Grabowski and M. Małecka, "Intramolecular H-bonds: DFT and QTAIM studies on 3-(aminomethylene)pyran-2, 4-dione and its derivatives," *Journal of Physical Chemistry A*, vol. 110, no. 42, pp. 11847–11854, 2006.

[44] S. J. Grabowski, "Ab initio calculations on conventional and unconventional hydrogen bonds-study of the hydrogen bond strength," *Journal of Physical Chemistry A*, vol. 105, no. 47, pp. 10739–10746, 2001.

[45] E. Espinosa, C. Lecomte, N. E. Ghermani et al., "Hydrogen bonds: First quantitative agreement between electrostatic potential calculations from experimental X-(X + N) and theoretical ab initio SCF models," *Journal of the American Chemical Society*, vol. 118, no. 10, pp. 2501–2502, 1996.

[46] B. Galabov and P. Bobadova-Parvanova, "Molecular electrostatic potential as reactivity index in hydrogen bonding: ab initio molecular orbital study of complexes of nitrile and carbonyl compounds with hydrogen fluoride," *Journal of Physical Chemistry A*, vol. 103, no. 34, pp. 6793–6799, 1999.

[47] V. Dimitrova, S. Ilieva, and B. Galabov, "Electrostatic potential at atomic sites as a reactivity descriptor for hydrogen bonding. Complexes of monosubstituted acetylenes and ammonia," *Journal of Physical Chemistry A*, vol. 106, no. 48, pp. 11801–11805, 2002.

[48] I. Mata, E. Molins, I. Alkorta, and E. Espinosa, "Topological properties of the electrostatic potential in weak and moderate N$\cdots$H hydrogen bonds," *Journal of Physical Chemistry A*, vol. 111, no. 28, pp. 6425–6433, 2007.

[49] P. Politzer, J. S. Murray, and M. C. Concha, "Halogen bonding and the design of new materials: organic bromides, chlorides and perhaps even fluorides as donors," *Journal of Molecular Modeling*, vol. 13, no. 6-7, pp. 643–650, 2007.

[50] P. W. Kenny, "Hydrogen bonding, electrostatic potential, and molecular design," *Journal of Chemical Information and Modeling*, vol. 49, no. 5, pp. 1234–1244, 2009.

[51] D. J. R. Duarte, M. M. de las Vallejos, and N. M. Peruchena, "Topological analysis of aromatic halogen/hydrogen bonds by electron charge density and electrostatic potentials," *Journal of Molecular Modeling*, vol. 16, no. 4, pp. 737–748, 2010.

[52] J. S. Murray, J. M. Seminario, M. C. Concha, and P. Politzer, "An analysis of molecular electrostatic potentials obtained by a local density functional approach," *International Journal of Quantum Chemistry*, vol. 44, no. 2, pp. 113–122, 1992.

[53] G. Chałasiński and M. M. Szczęśniak, "State of the art and challenges of the ab initio theory of intermolecular interactions," *Chemical Reviews*, vol. 100, no. 11, pp. 4227–4252, 2000.

[54] A. J. Stone, *The Theory of Intermolecular Forces*, Clarendon Press, Oxford, UK, 1996.

[55] S. Tsuzuki and A. Fujii, "Nature and physical origin of CH/π interaction: significant difference from conventional hydrogen bonds," *Physical Chemistry Chemical Physics*, vol. 10, no. 19, pp. 2584–2594, 2008.

[56] H. L. Williams and C. F. Chabalowski, "Using Kohn-Sham orbitals in symmetry-adapted perturbation theory to investigate intermolecular interactions," *Journal of Physical Chemistry A*, vol. 105, no. 3, pp. 646–659, 2001.

[57] R. Bukowski, K. Szalewicz, and C. F. Chabalowski, "Ab initio interaction potentials for simulations of dimethylnitramine solutions in supercritical carbon dioxide with cosolvents," *Journal of Physical Chemistry A*, vol. 103, no. 36, pp. 7322–7340, 1999.

[58] D. Kim, S. Hu, P. Tarakeshwar, K. S. Kim, and J. M. Lisy, "Cation-π interactions: a theoretical investigation of the interaction of metallic and organic cations with alkenes, arenes, and heteroarenes," *Journal of Physical Chemistry A*, vol. 107, no. 8, pp. 1228–1238, 2003.

[59] A. L. Ringer, M. S. Figgs, M. O. Sinnokrot, and C. D. Sherrill, "Aliphatic C-H/π interactions: methane-benzene, methane-phenol, and methane-indole complexes," *Journal of Physical Chemistry A*, vol. 110, no. 37, pp. 10822–10828, 2006.